UC Irvine

UC Irvine Previously Published Works

Title

Enhanced cytotoxic effects of 5-aminolevulinic acid-mediated photodynamic therapy by concurrent hyperthermia in glioma spheroids

Permalink

https://escholarship.org/uc/item/5zt1b9k3

Journal

Journal of Neuro-Oncology, 70(3)

ISSN

0167-594X

Authors

Hirschberg, Henry
Sun, Chung-Ho
Tromberg, Bruce J
et al.

Publication Date

2004-12-01

DOI

10.1007/s11060-004-9161-7

Copyright Information

This work is made available under the terms of a Creative Commons Attribution License, available at https://creativecommons.org/licenses/by/4.0/

Peer reviewed

eScholarship.org Powered by the California Digital Library
University of California


Journal of Neuro-Oncology **70:** 289–299, 2004.
© 2004 *Kluwer Academic Publishers. Printed in the Netherlands.*

Laboratory Investigation

Enhanced cytotoxic effects of 5-aminolevulinic acid-mediated photodynamic therapy by concurrent hyperthermia in glioma spheroids

Henry Hirschberg[1,2], Chung-Ho Sun[2], Bruce J. Tromberg[2], Alvin T. Yeh[2] and Steen J. Madsen[3,4]
[1]*Department of Neurosurgery, Rikshospitalet, Oslo, Norway;* [2]*Beckman Laser Institute and Medical Clinic, University of California, Irvine, USA;* [3]*Department of Health Physics, University of Nevada;* [4]*University of Nevada, Las Vegas Cancer Institute, Las Vegas, NV, USA*

Key words: 5-aminolevulinic acid, glioma, hyperthermia, photodynamic therapy, spheroid, synergism

Summary

During photodynamic therapy (PDT) both normal and pathological brain tissue, in close proximity to the light source, can experience significant temperature increases. The purpose of this study was to investigate the anti-tumor effects of concurrent 5-aminolevulinic acid (ALA)-mediated PDT and hyperthermia (HT) in human and rat glioma spheroids.

Human or rat glioma spheroids were subjected to PDT, HT, or a combination of the two treatments. Therapies were given concurrently to simulate the conditions that will occur during patient PDT.

Predictions of diffusion theory suggest that brain tissue immediately adjacent to a spherical light applicator may experience temperature increases approaching 8 °C for laser input powers of 2 W. In the *in vitro* model employed here, HT had no effect on spheroid survival at temperatures below 49 °C, while sub-threshold fluence PDT results in only modest decrease in survival. HT (40–46 °C) and PDT interact in a synergistic manner if the two treatments are given concurrently. The degree of synergism increases with increasing temperature and light fluence. Apoptosis is the primary mode of cell death following both low-fluence rate PDT and combined HT + PDT

Introduction

Primary brain tumors are neoplasms that originate from the parenchymal elements of the brain. There are approximately 17,000 new cases of primary brain tumors diagnosed within the United States every year and an equal number in the EU region [1]. Approximatly 40% of these are of the most malignant variety, glioblastoma multiforme (GBM). Five-year survival rates are dismal (<5%). Although viable tumor cells can be demonstrated in biopsy material remote from the primary tumor site, failure of treatment is usually due to local recurrence at the site of surgical resection [2]. This would indicate that although not curative, a more aggressive local therapy could be of benefit in prolonging patient survival and quality of life. Intracavity therapy offers the possibility of applying various treatment modalities (brachy, photodynamic and thermal therapies) aimed at the nests of tumor cells left in the resection border while minimizing damage to normal tissue [3–5].

Photodynamic therapy (PDT) of cancer involves the utilization of a tumor-localizing photosensitizing agent that, upon activation by light, results in the destruction of neoplastic tissue [6,7]. Since the efficacy of PDT depends, in part, on the ability to deliver adequate light doses to malignant cells in the resection margin, intraoperative treatment is unlikely to be effective due to the inability to deliver threshold light doses in a reasonable time period [8,9]. HT, the elevation of tissue temperature to at least 42 °C, has been used in combination with other treatment modalities in therapy for brain tumors [10,11]. HT kills cells as a function of temperature and time, inhibits repair of sub-lethal damage and makes hypoxic cells more vulnerable to radiation or PDT [12,13].

Due to the rapid attenuation of light in brain tissues [14–16], high laser powers are required to achieve threshold light fluences at cm depths in the resection margin. Since most of the optical energy is converted to heat, tissues in close proximity to the light source are likely to undergo significant heating. The effects of HT and PDT have been investigated in a number of *in vitro* [17–22] and *in vivo* [23–31] systems. Variable effects have been reported following combined HT and PDT, with the degree and type of interaction dependent on a number of factors including tumor type, treatment sequence, time interval between treatments and photosensitizer type [17–31]. Few of these studies though were done on normal brain or brain tumor tissue. Since HT is an unavoidable effect of high-fluence rate PDT [32], the present study was initiated to determine tumor cell-specific effects of the combined modalities in a human glioma spheroid model. To our knowledge, the combined effects of ALA-PDT and HT have not been investigated in such a model. Spheroids were used since cells in different locations in the spheroid experience different environments, thus mimicking the gradients found in solid tumors. In contradistinction to more complex animal models, spheroids allow for direct monitoring of the anti-tumor cell effects of treatment, separated from the influence of tumor vasculature, immunological reactions and other *in vivo* effects.

Materials and methods

Theoretical thermal distribution in the brain

A simple diffusion model was used to predict the thermal distribution in brain tissues during PDT with a spherical light applicator. Details of the model have been published elsewhere [32]. Briefly, temperature distributions in brain tissue depend on blood flow, applicator size, distance from the applicator to the point of interest, and on the thermal and optical properties of brain tissue. During PDT, a predominant part of the optical energy is converted to heat through tissue absorption. Since the thermal relaxation time (ca. 5–15 min) is typically an order of magnitude less than the total treatment time, the temperature distribution will be close to the steady-state values for most of the exposure period. Furthermore, since the dimensions of the tissue are much larger than the optical and thermal penetration depths, the medium can be considered as infinitely large in extent [33].

Cell cultures

Two different cell line-derived spheroids were used in this study. The human grade IV GBM cell line (ACBT) was a generous gift of G. Granger (University of California, Irvine, USA) [34]. The ACBT cells were cultured in DMEM (Gibco, Carlsbad, CA) with high glucose and supplemented with 2 mM L-glutamine, penicillin (100 U ml^{-1}), streptomycin (100 μg ml^{-1}), and 10% heat-inactivated fetal bovine serum (Gibco, Carlsbad, CA). The BT_4C cell line was derived originally from transformed fetal rat brain cells after exposure to ethylnitrosourea [35]. The BT_4C cells were grown as monolayers in RPMI medium with 10% heat-inactivated newborn calf serum (FCS) at 37 °C and 5% CO_2. The cell line tested negative for viral agents in a rat antibody production test according to the Federation of Laboratory Animal Association recommendations. Cells were maintained at 37 °C in a 7.5% CO_2 incubator. At a density of 70% confluence, cells were removed from the incubator and left at room temperature for approximately 20 min. The resultant cell clusters (consisting of approximately 10 cells) were transferred to a petri dish and grown to tumor spheroids using a liquid-overlay technique [36]. Spheroids in a range of 300–500 μm diameter were selected by passage through a screen mesh (Sigma, St. Louis, MO). It took approximately 21 days for spheroids to reach a size of 500 μm. The spheroid culture medium was changed three times weekly.

PDT and HT treatments

Human or rat spheroids were incubated in 100 or 500 μg ml^{-1} ALA (Sigma, St. Louis, MO) respectivly for approximately 4 h. In all cases, spheroids were irradiated with 635 nm light from an argon ion-pumped dye laser (Coherent, Inc., Santa Clara, CA). Light was coupled into a 200 μm dia. optical fiber containing a micro-lens at the output end. Spheroids were irradiated in a petri dish containing 400 μl of culture medium. The spheroids were confined to the central portion

of the dish to insure temperature uniformity and to limit the extent of the irradiated field. PDT was performed in a temperature-controlled incubator with the petri dishes placed on large metal blocks which had reached temperature equilibrium at 37, 40, 43, 46, or 49 °C. Temperatures chosen for the HT experiments were based on diffusion theory calculations of thermal distributions in brain tissues during PDT with spherical light applicators [8].

Temperatures were measured with thermocouples placed in parallel dishes containing no spheroids but an equal amount of culture medium. Temperature equilibrium was attained 15–20 min following placement of the culture medium in the incubator. PDT-only spheroids were irradiated at 37 °C, while HT dark controls were incubated in ALA but received no light. PDT-treated spheroids were irradiated to various fluences of 12–100 J cm^{-2} using a fluence rate of 25 mW cm^{-2}. Total irradiation times were between 8 and 64 min. In all cases, HT dark controls and PDT-treated spheroids were incubated at each temperature for a minimum of 40–45 min.

Following treatment (single or combined), individual spheroids were placed into separate wells of a 48-well culture plate and monitored for growth. Determination of spheroid size was carried out by measuring two perpendicular diameters of each spheroid using a microscope with a calibrated eyepiece micrometer. Typically, 24 spheroids were followed in each trial. Since each trial was performed 2 or 3 times, a total of 48–72 spheroids were followed for a given set of parameters. Spheroids were observed for up to 4 weeks.

The degree of interaction between the two treatment modalities was evaluated by a technique proposed by Drewinko et al. [37]. In this scheme, the degree of interaction is given by

$$\alpha = \frac{SF^{h} \times SF^{p}}{SF^{hp}}, \tag{1}$$

where SF^{h} and SF^{p} represent the surviving fractions with HT and PDT, respectively, and SF^{hp} is the surviving fraction following combined treatments. In this analysis, $\alpha = 1$ indicates an additive effect (or absence of any effect), $\alpha > 1$ indicates a synergistic effect, and $\alpha < 1$ indicates an antagonistic effect.

TUNEL assay

The presence of apoptosis was evaluated using a TUNEL assay. Approximately 24 h after treatment, the spheroids were removed from the well plates and fixed in 2% formaldehyde for 24 h. The spheroids were washed three times in phosphate-buffered saline and subjected to the DeadEnd TM flourometric terminal deoxynucleotidyl transferase (TdT) – mediated deoxyuridine triphosphate nick-end labeling system (Promega Corp., Madison, WI) – a classic TUNEL assay that measures nuclear DNA fragmentation in apoptotic cells by incorporating fluorescein-12-deoxyuridine triphosphate at 3′-OH DNA ends using the enzyme TdT. In comparison to nuclear morphology techniques, this assay has been shown to have a higher degree of accuracy for the detection of apoptosis [38] and, as such, has been used to quantify programmed cell death in a number of brain tumor cell lines [39,40]. The fluorescein label was detected by two-photon fluorescence microscopy [41]. The fluorescein was excited at a wavelength of 400 nm, and the resultant fluorescence images were collected using a long-pass (530 nm cut-off) filter (CVI, Albuquerque, NM). Images were acquired over spheroid depths ranging from 30 to 100 μm. Depth discrimination was accomplished by adjusting the Z position of the 10X (0.3 numerical aperture (NA)) objective (Zeiss, Thornwood, NY). Image acquisition times were of the order of 15 s (10 frames at 1.5 frames s^{-1}).

The total number of apoptotic cells in each image was determined by counting the number of fluorescing nuclei. The apoptotic fraction (AF) was determined from

$$AF = \frac{N_f}{N_t}, \tag{2}$$

where N_f is the number of fluorescing nuclei, and N_t is the total number of cells in the field of view (200 μm × 200 μm). To determine the total number of cells, control spheroids were stained with 100 μg ml^{-1} 4,6-diamidino-2-phenylindole, dihydrochloride (DAPI; Molecular Probes, Inc., Eugene, OR) – a nucleic acid stain that associates with the minor groove of double-strand DNA, preferentially binding to AT base pairs. Excitation of bound DAPI ($\lambda_{peak} = 370$ nm) results in blue fluorescence ($\lambda_{peak} = 465$ nm). DAPI fluorescence

was imaged using the two-photon fluorescence microscope system.

Selected spheroids (positive controls) were exposed to deoxyribonuclease I which mimics apoptosis by inducing fragmentation of chromosomal DNA. The resultant exposed 3′-OH DNA ends were labeled with fluorescein and imaged as described previously. Negative controls denote spheroids that were not subjected to any treatment. They represent the ambient level of apoptosis in this *in vitro* system. The AF was determined for three spheroids in each control or treatment group. Because each treatment was repeated, the AF was averaged over six spheroids.

Results

Thermal distribution calculations

Temperature distributions from balloon-type spherical applicators are illustrated in Figure 1. As expected, the maximum temperature (T_{max}) occurs at the surface of the applicator. Furthermore, for a given input power, T_{max} increases with decreasing applicator diameter. Since T_{max} scales linearly with input power, the input power required for a rise in T_{max} of 8 °C (the hyperthermic threshold) can be determined in a relatively straightforward manner. The input powers resulting in a rise in T_{max} of 8 °C, are shown in Table 1. The input powers in Table 1 correspond to maximum treatment depths of 1.4 cm [8].

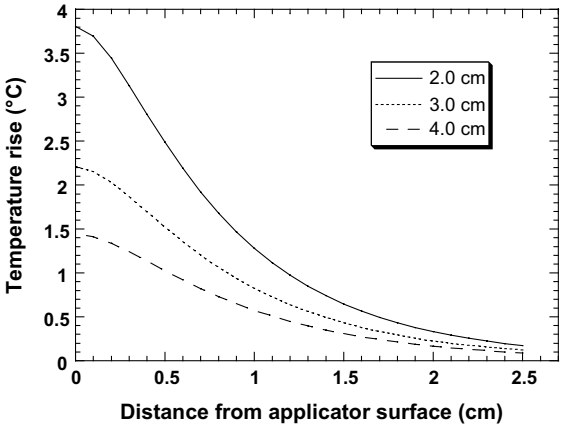

Figure 1. Calculated temperature rise in brain tissue for a 1 W input power. Thermal distributions are shown for three different spherical applicator diameters.

Table 1. Input power resulting in a T_{max} rise of 8 °C

Applicator diameter (cm)	Input power (W)
2.0	2.1
3.0	3.6
4.0	5.7

Effects of either HT or PDT on glioma spheroids

The effects of either hyperthermia or PDT on human ACBT and rat BT_4C spheroid survival are summarized in Figure 2. The control group spheroids (37 °C) received no light (dark controls) but were incubated in ALA for 4 h and subjected to temperatures of 37 °C for 30 min. Two other control groups (light only, and no drug/no light) exhibited survival (100%) identical to that observed for the dark controls (data not shown). Figure 2 also shows that relatively high temperatures are required for a significant cytotoxic response – the temperature required for 5% survival

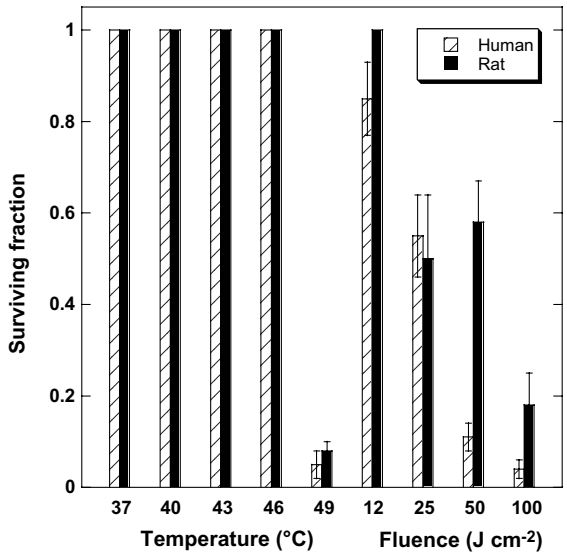

Figure 2. Effects of HT or PDT on human and rat BT_4C spheroid survival measured 4 weeks post-treatment. Light fluences in the range of 25–100 J cm^{-2} were delivered using a fluence rate of 25 mW cm^{-2}. Each data point represents the mean (± SE) of 48–56 spheroids.

is approximately 49 °C. No significant spheroid kill was observed at temperatures up to 46 °C. Since the accuracy of the temperature measurements was of the order of 1 degree, no attempt was made to determine survival rates in the interval between 46 and 49 °C. As illustrated in Figure 2, low-fluence PDT at 37 °C is relatively ineffective, resulting in spheroid survivals of approximately 90 and 60% at fluences of 12 and 25 J cm^{-2}, respectively for the human spheroids. These fluences were chosen since they have been shown to be sub-optimal in this system [42]. Similar results were also obtained for spheroids grown from BT_4C cells, with temperatures below 49 °C showing no inhibitory effects (Figure 2). The rat spheroids at 37 °C were more resistant to PDT compared to the human ones. At a total fluence of 50 J cm^{-2} approximately 60% survived compared to 11% for human spheroids.

Effects of combined PDT and HT on the kinetics of human spheroid growth

As shown in Figure 3, sub-lethal temperatures appear to have no effect on spheroid growth – the growth kinetics of spheroids subjected to 46 and 37 °C are identical. In contrast, sub-lethal light fluences appear to have a significant inhibitory effect on spheroid growth. This effect is fluence dependent as a greater growth delay is observed for the higher fluence. The growth delay induced by the combination of HT and PDT is also shown. The doubling time for spheroids treated with PDT at 46 °C was greater than 28 days. In contrast, the doubling time for the 46 °C exposed spheroids was approximately 8 days – identical to that observed at 37 °C. Similar results were obtained with BT_4C derived spheroids (data not shown).

Effects of combined PDT and HT on spheroid survival

A significant inhibitory response was observed in both human and rat glioma spheroids subjected to concurrent HT and PDT (Figures 4 and 5). The degree of response is clearly temperature and fluence dependent below 49 °C – treatment efficacy improves with increasing temperature and light fluence.

The degree of interaction between the two modalities, as indicated by the α coefficient, is summarized in Figure 6 for human spheroids. At temperatures below 49 °C, HT and PDT interact in a synergistic manner ($\alpha > 1$) if the two treatments

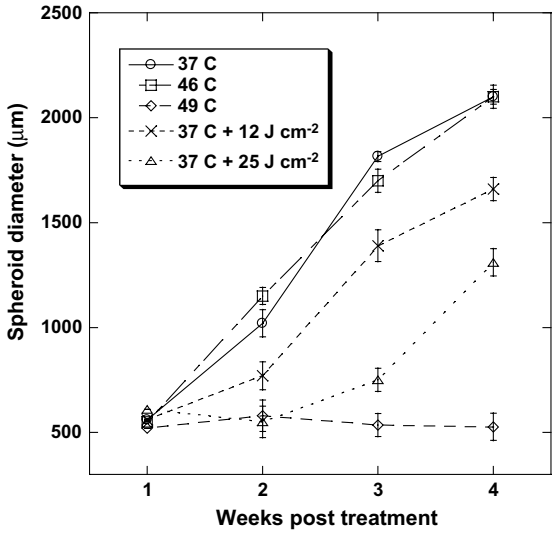

Figure 3. Effects of HT, PDT, or HT + PDT on human spheroid growth. In all PDT treatments, a fluence rate of 25 mW cm^{-2} was used. Each data point represents the mean (± SE) of 48–56 spheroids.

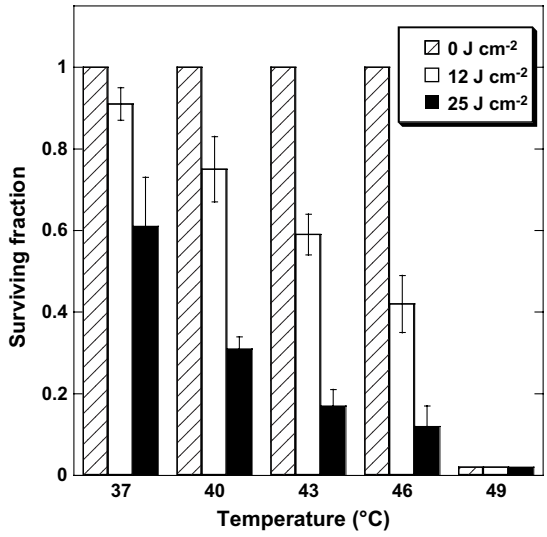

Figure 4. Effects of concurrent PDT and HT on human spheroid survival. The HT-only spheroids (0 J cm^{-2}) were incubated in 100 μg ml^{-1} ALA 4 h prior to treatment. In all PDT treatments, a fluence rate of 25 mW cm^{-2} was used. Each data point represents the mean (± SE) of 56–72 spheroids.

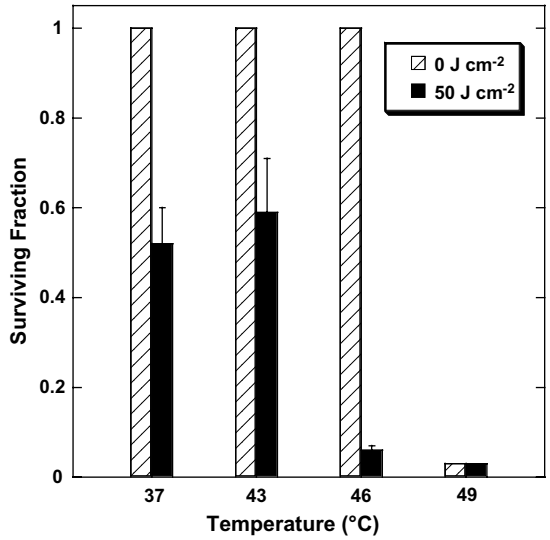

Figure 5. Effects of concurrent PDT and HT on rat (BT_4C) spheroid survival. The HT-only spheroids ($0\,J\,cm^{-2}$) were incubated in $500\,\mu g\,ml^{-1}$ ALA 4 h prior to treatment. In all PDT treatments, a fluence rate of $25\,mW\,cm^{-2}$ to a total fluence of $50\,J\,cm^{-2}$ was used. Each data point represents the mean ($\pm$SE) of 56–72 spheroids.

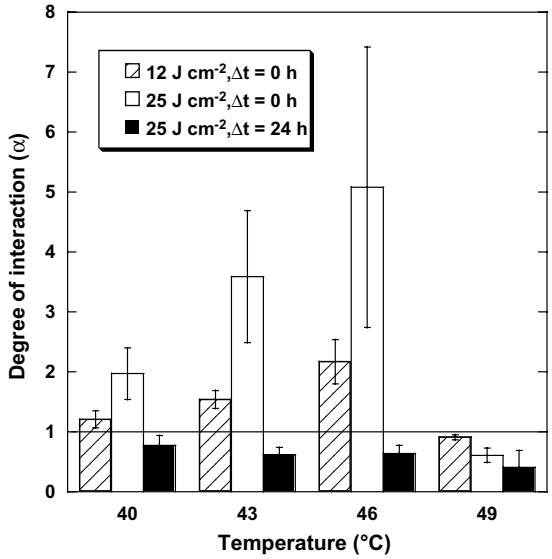

Figure 6. Degree of interaction between HT and PDT as a function of temperature on human spheroids. Three cases are considered: concurrent HT and PDT ($\Delta t = 0$) at two light fluences, and HT given 24 h prior to PDT ($\Delta t = 24$ h). In all PDT treatments, a fluence rate of $25\,mW\,cm^{-2}$ was used. The horizontal line denotes the boundary between synergism ($\alpha > 1$) and antagonism ($\alpha < 1$). Each data point represents the mean ($\pm$ SE) of 48–72 human spheroids.

are given concurrently. The highest degree of potentiation ($\alpha \approx 5$) is obtained at a temperature and fluence of 46 °C and $25\,J\,cm^{-2}$, respectively. In all cases, the introduction of a 24 h delay between the two treatments results in a decreased PDT effect as indicated by α coefficients below unity.

Determination of the mode of spheroid growth inhibition

In order to gain insight into the mechanism(s) of synergism, the mode of cell death was determined as a function of treatment modality. The ability of various treatments to induce apoptosis in the cells comprising the human spheroids is illustrated in Figure 7. It is shown that low-fluence rate PDT is a very effective inducer of apoptosis – the AF (ca. 0.9) for PDT at 37 °C is comparable to that observed in the positive controls (data not shown). In contrast, HT is a very poor inducer of apoptosis – the AF (ca. 5%) is equivalent to that observed in the negative controls (data not shown). Spheroids subjected to concurrent HT and PDT showed similar levels of apoptosis as those subjected to PDT only. Interestingly, PDT given at 49 °C, a degree of HT

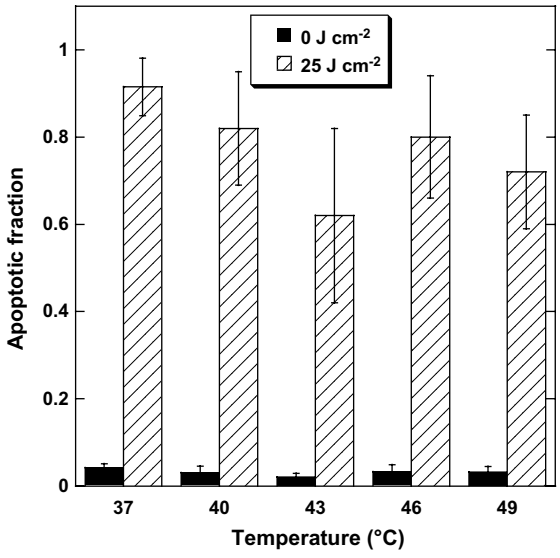

Figure 7. Fraction of cells in human spheroids showing apoptosis as a function of treatment type. The AF was evaluated from two-photon fluorescence images (10X) acquired at a spheroid depth of approximately 60 μm. Each data point represents the mean of 6 spheroids from two independent treatments. Error bars denote standard deviations.

yielding 100% spheroid kill in the absence of light, also resulted in significant apoptosis. The absence of apoptosis in spheroids subjected to HT at 49 °C suggests a necrotic mode of cell death. Two-photon fluorescence images of representative human glioma spheroids are illustrated in Figure 8. In these false-colored images, the bright fluorescing centers represent nuclei that have incorporated fluorescein and, hence, have undergone apoptosis. The images clearly show significant induction of apoptosis following PDT and HT + PDT, while HT alone is a poor inducer of apoptosis.

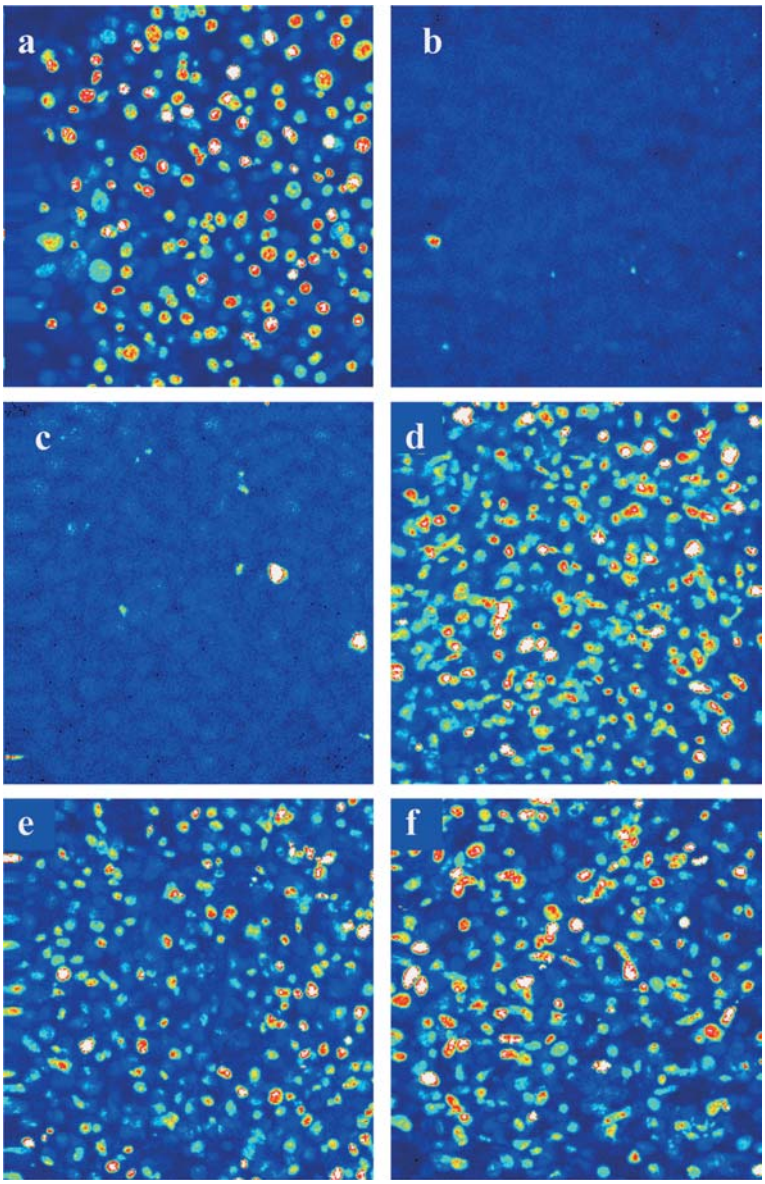

Figure 8. Two-photon fluorescence images (X–Y plane, $Z = 60\,\mu m$) of human glioma spheroids 24 h post-treatment. The dimension of each image is approximately 200 μm by 200 μm. A false color scale is used to denote fluorescein fluorescence intensity: white and red represent strong fluorescence while green and blue denote weakly fluorescing nuclei. (a) PDT (25 mW cm^{-2}, 25 J cm^{-2}), (b) HT (43 °C), (c) HT (49 °C), (d) HT (40 °C) + PDT, (e) HT (43 °C) + PDT and, (f) HT (49 °C) + PDT.

Discussion

The possibility of a synergistic effect between ALA-mediated PDT and HT prompted the present study since tissue heating is an unavoidable consequence of high-fluence rate light irradiations such as those required for PDT treatments of GBM cells residing deep in resection margins. Theoretical calculations indicate that significant temperature increases are likely to occur in brain tissue immediately adjacent to a spherical light applicator following even modest input laser powers (Figure 1). The higher input powers that are likely required for the elimination of GBM cells at 1–2 cm depths would result in even greater temperature increases, perhaps as high as 8 °C. It is imperative to keep temperatures below about 43 °C in order to avoid large-scale hyperthermic damage to normal brain tissues.

Both types of multicell spheroids used in this study appeared to be very thermoresistant – significant suppression was observed only at temperatures approaching 49 °C (Figure 2). Furthermore, in contrast to sub-optimal fluence PDT, HT at sub-threshold temperatures (<49 °C) had no observable effect on spheroid growth kinetics (Figure 3). In comparison, GBM cells in monolayer are sensitive to much lower temperatures – exposures to 44 °C results in significant cell kill [43]. The relative ineffectiveness of HT on GBM cells in spheroids, is likely due to the close three-dimensional contact between cells (the contact effect) which has been shown to confer increased resistance of cells to various therapies, including HT [44,45]. Although neither PDT nor HT was particularly effective, a significant reduction in spheroid survival was nevertheless observed when the two treatments were given concurrently (Figures 4 and 5). The efficacy of the combined treatment improved with increasing temperature and light fluence. As shown in Figure 6, the two treatment modalities interacted synergistically at all temperatures below 49 °C. Not surprisingly, the degree of synergism was observed to increase with increasing temperature and light fluence.

In order to gain insight into the mechanism(s) of synergism, the mode of cell death was determined as a function of treatment modality. As illustrated in Figures 7 and 8, HT is a poor inducer of apoptosis in GBM cells. The inability of HT to induce apoptosis in this cell line is likely due to the high constitutive expression of heat shock proteins (HSPs) in GBM cells [46]. Apoptosis and induction of HSPs have been found to be mutually exclusive due to the protective effect of HSPs [47]. Due to the inability of HT to induce apoptosis, the observed cell death at 49 °C was attributed to necrosis. This is in good agreement with the findings of others that necrosis is the predominant mode of cell death following exposures to high temperatures [48].

Low-fluence rate ALA-PDT has been shown to induce apoptosis in the human glioma cell line investigated in this study [49]. This is confirmed in the present study which shows that apoptosis is the primary mode of cell death following exposure to low-fluence rate PDT at all temperatures investigated, including 49 °C, a temperature that resulted in pronounced cytotoxicity in the absence of light. Since the cytotoxic effects of HT at 49 °C are likely due to necrosis, the addition of PDT would appear to have the effect of switching the cells to an apoptotic mode of cell death. Although the details of this effect are unknown, the clinical implications are potentially significant since lower levels of brain edema are thought to be present following apoptosis-inducing therapies compared to those in which necrosis is the primary mode of cell death.

In spite of the high levels of apoptosis observed following low fluence rate PDT (Figure 7), the treatment was relatively ineffective as evidenced by the high spheroid survival shown in Figure 4. This apparent contradiction can be explained by the fact that apoptosis was evaluated under well-oxygenated conditions such as those present in the superficial layer of the spheroid. Since PDT is an oxygen-dependent treatment modality, the well-oxygenated cells in the superficial layer will be particularly susceptible to its effects – apoptosis in the case of low-fluence rate ALA-mediated PDT [42]. However, due to limited oxygen diffusion, cells far from the surface (>100 μm) may be spared the cytotoxic effects of PDT thus resulting in renewed spheroid growth. Thus, even though apoptosis is the primary effect of low fluence rate ALA-mediated PDT in the glioma cells studied in this work, the effectiveness of this treatment modality is relatively poor since the effect does not extend to all viable cells of the spheroid.

Although the mechanism of synergism between PDT and HT is not known, it likely has several components. For instance, it might be due, in part,

to photodynamically induced inhibition of cellular repair following sub-lethal thermal damage [17]. Another hypothesis for the observed synergism is the concerted action of both treatment modalities on cellular proteins [20]. For example, it has been shown that PDT can result in the photooxidation of intracellular enzymes such as glyceraldehyde-3-phosphate dehydrogenase and cytochrome c oxidase [50]. As a result, the enzymes undergo a conformational change which, in turn, affects their susceptibility for thermal inactivation. The net effect of PDT is thus to lower the activation energy of protein denaturation, thus making the proteins more susceptible to thermal damage. The observation of high levels of apoptotic cell death following combined HT and PDT (Figure 7) is consistent with this hypothesis since these proteins can be found in the mitochondrial membrane and ALA-induced protoporphyrin IX has significant mitochondrial localization [51]. In other words, ALA-induced PDT may result in significant damage to proteins in the mitochondrial membrane thus making them more susceptible to thermal inactivation. Damage to these proteins would presumably result in damage to the mitochondrial membrane thus increasing the likelihood of apoptosis.

Although the effects of combining PDT and HT are dependent on the timing of the two modalities [18, 27, 30] the main purpose of the experiments reported here was to examine the effects of concurrent PDT and HT, since this would simulate a clinical protocol.

Conclusions

In summary, the addition of concurrent HT appears to be an efficient strategy to increase the antitumor effect of ALA-mediated PDT in the therapy of gliomas. Although the mechanisms of synergism remain to be clarified, they may be due, in part, to a common mode of action on cellular proteins.

Acknowledgements

Steen Madsen is grateful for the support of the UNLV Office of Research and the UNLV Cancer Institute. Henry Hirschberg is grateful for the support of the Norwegian Cancer Society and the Norwegian Research Council. This work was made possible, in part, through access to the Laser Microbeam and Medical Program (LAMMP) and the Chao Cancer Center Optical Biology Shared Resource at the University of California, Irvine. These facilities are supported by the National Institutes of Health under grants RR-01192 and CA-62203, respectively. In addition, Beckman Laser Institute programmatic support was provided by the Department of Energy (DOE #DE-FG03-91ER61227), and the Office of Naval Research (ONR #N00014-91-C-0134).

References

1. Salcman M: Epidemiology and factors affecting survival. In: Apuzzo MLJ (ed) Malignant Cerebral Glioma. Amercian Association of Neurological Surgeons, Park Ridge, IL, 1990, pp 95–109
2. Wallner KE, Galicich JH, Krol G, Arbit E, Malkin MG: Patterns of failure following treatments for glioblastoma multiforme and anaplastic astrocytoma. Int J Radiat Oncol Biol Phys 16: 1405–1409, 1989
3. Ashpole R, Syndman H, Bullimore A: A new technique of brachytherapy for malignant glioma with cesium-137. Clin Oncol 2: 333–337, 1990
4. Johannesen TB, Watne K, Lote K, Norum J, Henning R, Tveraa K, Hirschberg H: Intracavity fractionated balloon brachytherapy in glioblastoma. Acta Neurochir (Wien) 141: 127–133, 1999
5. Muller PJ, Wilson BC: Photodynamic therapy: cavitary photoillumination of malignant cerebral tumours using a laser coupled inflatable balloon. Can J Neurol Sci 12(4): 371–381, 1985
6. Dougherty TJ, Gomer CJ, Henderson BW, Jori G, Kessel D, Korbelik M, Moan J, Peng Q: Photodynamic therapy. J Natl Cancer Inst 90: 889–905, 1998
7. Sharman WM, Allen CM, van Lier JE: Photodynamic therapeutics: basic principles and clinical applications. Drug Discov Today 4: 507–517, 1999
8. Madsen SJ, Svaasand LO, Tromberg BJ, Hirschberg H: Characterization of optical and thermal distributions from an intracranial balloon applicator for photodynamic therapy. In: Duncan DD, Jacques SL, Johnson PC (eds) Laser-Tissue Interaction XII: Photochemical, Photothermal and Photomechanical, Proceedings SPIE, Vol. 4257, SPIE Publishers, Bellingham, WA, 2001, pp 41–49
9. Madsen SJ, Sun C-H, Tromberg BJ, Hirschberg H: Development of a novel balloon applicator for optimizing light delivery in photodynamic therapy. Lasers Surg Med 29: 406–412, 2001
10. Sneed PK, Gutin P, Stauffer PR, Phillips TL, Prados MD, Weaver KA, Suen S, Lamb SA, Ham B, Ahn DK,

Lamborn K, Larson DA, Wara WM: Thermoradiotherapy of recurrent malignant brain tumors. Int J Radiat Oncol Biol Phys 23: 853–861, 1992
11. Stea B, Kittelson J, Cassady JR, Hamilton A, Guthkelch N, Lulu B, Obbens E, Rossman K, Shapiro W, Shetter A, Cetas T: Treatment of malignant gliomas with interstitial irradiation and hypethermia. Int J Radiat Oncol Biol Phys 24: 657–667, 1992
12. Oleson JR: Hyperthermia from the clinic to the laboratory: a hypothesis. Int J Hyperthermia 11: 315–322, 1995
13. Dewey WC, Freeman ML, Raaphorst GP, Clark EP, Wong RSL, Highfield DP, Spiro IJ, Tomasovic S, Denman DL, Cross RA: Cell biology of hyperthermia and radiation. In: Meyn RE, Withers HR (eds) Radiation Biology in Cancer Research. Raven Press, New York, 1980, pp 89–621
14. Svaasand LO, Ellingson R: Optical properties of human brain. Photochem Photobiol 38: 293–299, 1983
15. Svaasand LO, Ellingson R: Optical penetration in human intracranial tumors. Photochem Photobiol 41: 73–76, 1985
16. Wilson BC, Muller PJ: An update on the penetration depth of 630 nm light in normal and malignant human brain tissue *in vivo*. Phys Med Biol 31: 1295–1297, 1986
17. Christensen T, Wahl A, Smedshammer L: Effects of haematoporphyrin derivative and light in combination with hyperthermia on cells in culture. Br J Cancer 50: 85–89, 1984
18. Mang TS, Dougherty TJ: Time and sequence dependent influence of *in vitro* photodynamic therapy survival by hyperthermia. Photochem Photobiol 42: 533–540, 1985
19. Miyoshi N, Matsumoto N, Hisazumi H, Fukuda M: The effect of hyperthermia on murine leukaemia cells in combination with photodynamic therapy. Int J Hyperthermia 4: 203–209, 1988
20. Prinsze C, Penning LC, Dubbelman TMAR, VanSteveninck J: Interaction of photodynamic treatment and either hyperthermia or ionizing radiation and of ionizing radiation and hyperthermia with respect to cell killing of L929 fibroblasts, Chinese hamster ovary cells and T24 human bladder carcinoma cells. Cancer Res 52: 117–120, 1992
21. Rasch MH, Tijssen K, VanSteveninck J, Dubbelman TMAR: Synergistic interaction of photodynamic treatment with the sensitizer aluminum phthalocyanine and hyperthermia on loss of clonogenicity of CHO cells. Photochem Photobiol 64: 586–593, 1996
22. Chen B, Xu Y, Agostinis P, DeWitte PAM: Synergistic effect of photodynamic therapy with hypericin in combination with hyperthermia on loss of clonogenicity of RIF-1 cells. Int J Oncology 18: 1279–1285, 2001
23. Henderson BW, Waldow SM, Potter WR, Dougherty TJ: Interaction of photodynamic therapy and hyperthermia: tumor response and cell survival studies after treatment of mice *in vivo*. Cancer Res 45: 6071–6077, 1985
24. Waldow SM, Henderson BW, Dougherty TJ: Hyperthermic potentiation of photodynamic therapy employing photofrin I and II: comparison of results using three animal models. Lasers Surg Med 7: 12–22, 1987
25. Mang TS: Combination studies of hyperthermia induced by the Neodymium: Yttrium–Aluminum–Garnet (Nd:YAG) laser as an adjuvant to photodynamic therapy. Lasers Surg Med 10: 173–178, 1990
26. Jiang Q, Chopp M, Hetzel FW: *In vivo* ^{31}P NMR study of combined hyperthermia and photodynamic therapies of mammary cell carcinoma in the mouse. Photochem Photobiol 54: 795–799, 1991
27. Kimel S, Svaasand LO, Hammer-Wilson M, Gottfried V, Cheng S, Svaasand E, Berns MW: Demonstration of synergistic effects of hyperthermia and photodynamic therapy using the chick chorioallantoic membrane model. Lasers Surg Med 12: 432–440, 1992
28. Dereski MO, Madigan L, Chopp M: The effect of hypothermia and hyperthermia on photodynamic therapy of normal brain. Neurosurgery 36: 141–146, 1995
29. Chen Q, Chen H, Shapiro H, Hetzel FW: Sequencing of combined hyperthermia and photodynamic therapy. Rad Res 146: 293–297, 1996
30. Liu DL, Andersson-Engels S, Sturesson C, Svanberg K, Haakansson CH, Svanberg S: Tumor vessel damage resulting from laser-induced hyperthermia alone and in combination with photodynamic therapy. Cancer Lett 111: 157–165, 1997
31. Chen B, Roskams T, deWitte PAM: Enhancing the antitumoral effect of hypericin-mediated photodynamic therapy by hyperthermia. Lasers Surg Med 31: 158–163, 2002
32. Svaasand LO: Temperature rise during photoirradiation therapy of malignant tumors. Med Phys 10: 10–17, 1983
33. Svaasand LO: Thermal distribution from inserted optical fibers. In: Waidelich W, Kiefhaber P (eds) Optoelectronics in Medicine: Proceedings of the 2nd International Nd:YAG Laser Conference. Springer-Verlag, Berlin, 1985, pp 294–301
34. Ross HJ, Canada AL, Antoniono RJ, Redpath JL: High and low dose rate irradiation have opposing effects on cytokine gene expression in human glioblastoma cell lines. Eur J Cancer 33: 144–152, 1997
35. Mella O, Bjerkvig R, Schem BC, Dahl O, Laerum OD: A cerebral glioma model for experimental therapy and in vivo invasion studies in syngeneic BD IX rats. J Neurooncol 9: 93–104, 1990
36. Sutherland RM, Carlsson J, Durand RE, Yuhas J: Spheroids in cancer research. Cancer Res 41: 2980–2994, 1981
37. Drewinko B, Loo TL, Brown B, Gottlieb JA, Freireich EJ: Combination therapy in vitro with adriamycin: observation of additive, antagonistic, and synergistic effects when used in two-drug combinations on cultured human lymphoma cells. Cancer Biochem Biophys 1: 187–195, 1976
38. Gavrieli Y, Sherman Y, Ben-Sasson SA: Identification of programmed cell death in situ via specific labeling of nuclear DNA fragmentation. J Cell Biol 19: 493–501, 1992
39. Ray SK, Wilford GG, Crosby CV, Hogan EL, Banik NL: Diverse stimuli induce calpain overexpression and apoptosis in C6 glioma cells. Brain Res 829: 18–27, 1999
40. Ray SK, Fidan M, Nowak MW, Wilford GG, Hogan EL, Banik EL: Oxidative stress and Ca^{2+} influx upregulate

calpain and induce apoptosis in PC12 cells. Brain Res 852: 326–334, 2000
41. Wallace VP, Dunn AK, Coleno ML, Tromberg BJ: Two photon microscopy in highly scattering tissue. In: Periasamy A (ed) Methods in Cellular Imaging. Oxford University Press, Cary, NC, 2001, pp 180–199
42. Madsen SJ, Sun C-H, Tromberg BJ, Wallace VP, Hirschberg H: Photodynamic therapy of human glioma spheroids using 5-aminolevulinic acid. Photochem Photobiol 72: 128–134, 2000
43. Takahisa F, Yoon K-W, Kato T, Kazuo Y: Heat-induced apoptosis in human glioblastoma cell line A172. Neurosurgery 42: 843–849, 1998
44. Olive PL, Durand RE: Drug and radiation resistance in spheroids: cell contact and kinetics. Cancer Metastasis Rev 13: 121–138, 1994
45. Wigle JC, Sutherland PM: Increased thermoresistance developed during growth of small multicellular spheroids. J Cell Physiol 122: 281–289, 1985
46. Hermisson M, Strik H, Rieger J, Dichgans J, Meyermann R, Weller M: Expression and functional activity of heat shock proteins in human glioblastoma multiforme. Neurology 54: 1357–1364, 2000
47. Gorman AM, Heavey B, Creagh E, Cotter TG, Samali A: Antioxidant-mediated inhibition of the heat shock response leads to apoptosis. FEBS Lett 445: 98–102, 1999
48. Harmon BV, Corder AM, Collins RJ, Gobe GC, Allen J, Allan DJ, Kerr JFR: Cell death induced in a murine mastocytoma by 42–47 °C heating *in vitro*: evidence that the form of death changes from apoptosis to necrosis above a critical heat load. Int J Radiat Biol 58: 845–858, 1990
49. Madsen SJ, Sun C-H, Tromberg BJ, Yeh AT, Sanchez R, Hirschberg H: Effects of combined photodynamic therapy and ionizing radiation on human glioma spheroids. Photochem Photobiol 76: 411–416, 2002
50. Prinsze C, Dubbelman TMAR, VanSteveninck J: Potentiation of the thermal inactivation of glyceraldehydes-3-phosphate dehydrogenase by photodynamic treatment. A possible model for the synergistic interaction between photodynamic therapy and hyperthermia. Biochem J 276: 357–362, 1991
51. Verma A, Facchina SL, Hirsch DJ, Song S-Y, Dillahey LF, Williams JR, Snyder SH: Photodynamic tumor therapy: mitochondrial benzodiazepine receptors as a therapeutic target. Mol Med 4: 40–48, 1998

Address for offprints: Steen J. Madsen, Department of Health Physics, University of Nevada, 4505 Maryland Pkwy., Box 453037, Las Vegas, NV 89154-3037, USA; Tel.: +1-702-895-1805; Fax: +1-702-895-4819; E-mail: steenm@ccmail.nevada.edu